JOURNAL OF MAGNETIC RESONANCE IMAGING 31:268–278 (2010)

Review

High Resolution Noncontrast MRI of the Hip

CME

Hollis G. Potter, MD,* and Jennifer Schachar, BA

The relatively thin cartilage of the hip joint, as well as its complex geometry, poses challenges for standardized, reproducible assessment of cartilage and the acetabular labrum. With appropriate pulse sequence parameters, however, accurate, reproducible assessment of cartilage and the labrum is feasible. More detailed evaluation of cartilage biochemistry may be obtained with techniques aimed at noninvasively evaluating the integrity of collagen and/or proteoglycan components in the articular cartilage. One of the benefits of noncontrast techniques lie in the ability to visualize the native synovium, and thereby detect the presence of synovial proliferative disorders, the clinical symptoms of which may mimic a labral tear or traumatic cartilage injury. Standard cartilage evaluation allows for the detection of surface delamination and osteoarthritis in the setting of femoroacetabular impingement, as well as subtle areas of subchondral collapse and secondary delamination of cartilage in the setting of osteonecrosis. This preserves the use of hip arthroscopy as a therapeutic rather than a diagnostic tool.

Key Words: hip; femoroacetabular impingement; cartilage; T2 mapping; dGEMRIC
J. Magn. Reson. Imaging 2010;31:268–278.

REPRODUCIBLE, ACCURATE ASSESSMENT of the hip joint using MRI is challenging, given the anatomic location of the hip joint from the isocenter of the imaging bore, as well as the relatively thin cartilage over the femoral head and dome. In addition, the curvilinear contour of the femoral head poses challenges for both morphologic and quantitative imaging of the articular surface. With appropriate attention to technique, however, reproducible assessment of the hip cartilage is possible, and may be obtained without the standardized use of intra-articular contrast agents. Due to the rapid rise in hip arthroscopic procedures, accurate preoperative evaluation of the hip joint is necessary. Given the tight intracapsular pressure of the joint, hip arthroscopy is technically challenging and there is a greater risk for iatrogenic damage to the articular surfaces, when compared with arthroscopy performed in the more patulous recesses of the knee or shoulder. Standardized preoperative MRI may then be used as the diagnostic tool, preserving hip arthroscopy as a technique more restricted to therapeutic management.

Hospital for Special Surgery, Weil Medical College of Cornell University, New York, NY, USA.

*Address reprint requests to: H.G.P., Hospital for Special Surgery, 535 East 70th Street, New York, NY 10021. E-mail: potterh@hss.edu

Received August 27, 2009; Accepted October 16, 2009.

DOI 10.1002/jmri.22025
Published online in Wiley InterScience (www.interscience.wiley.com).

IMAGING TECHNIQUE

Hip MRI is best performed on 1.5 or 3 Tesla (T) magnets. No truly dedicated hip coil exists, and hip imaging is thus best performed with either a two part shoulder coil, a smaller field of view wrap coil, or a multiple channel cardiac coil. The large field of view wrap body coils are unsuitable for hip imaging, as the necessary in-plane resolution will result in phase wrap. Coronal images should be obtained posterior to the hip joints, through the axis of the sciatic nerve, and anteriorly through the hip joint to the level of the iliopsoas. Moderate echo time fast spin echo sequencing with an effective echo of approximately 34 ms at 1.5T and 28 ms at 3T is recommended (Table 1). The inherent magnetization transfer contrast of fast or turbo spin echo techniques will yield differential contrast from the low signal fibrocartilaginous labrum, intermediate signal intensity articular cartilage, and high signal intensity fluid.

Coronal images demonstrate to best advantage the suprafoveal articular cartilage over the femoral head, lateral dome, and superior labrum. In addition, it is the optimal view for evaluation of the hip abductors, short external rotator tendon attachments, and the attachment of the iliopsoas to the lesser trochanter. Furthermore, the iliofemoral ligament is well visualized in the coronal view (Fig. 1).

Sagittal images are the optimal plane for evaluation of the anterior labrum. The majority of labral tears, in the absence of a posterior subluxation history, are localized in the anterior labrum (1). The importance of through-plane resolution is stressed in evaluation of the anterior labrum, particularly using noncontrast techniques. A slice thickness of 2–2.5 mm with no interslice gap is recommended to discern subtle splits. Additionally, the sagittal images afford reliable evaluation of the cartilage over the dome and the head. The sciatic nerve can also be visualized posterior to the hip joint.

Table 1
Recommended Protocols for MRI of the hip at 1.5 T. and 3.0 T

Recommended Hip MRI Protocol at 1.5T (Coil: body, phased array shoulder, Position: feet first supine, Landmark: femoral head)					
	Coronal fast inversion recovery (whole pelvis)	Axial FSE (whole pelvis)	Sagittal FSE (affected hip)	Coronal FSE (affected hip)	Oblique axial FSE (affected hip)
TR (msec)	3500–5000	4000–5000	4000–5000	4000–5000	4000–5000
TE (msec)	17	34	34	34	34
TI	150				
BW (kHz)	31.25	31.25	31.25	31.25	31.25
ETL	7–9	8–12	9–12	9–12	9–12
Flip (deg.)					
NEX	2	2	3	3	3
FOV (cm)	Greater inter-trochanteric distance plus 2cm	Greater inter-trochanteric distance	17–18	17–18	16
Matrix	256 × 192	512 × 256	512 × 384	512 × 384	512 × 256
Slice/Gap (mm)	5/0	5/0	2.5/0	4/0	3/0
NPW	✓	✓	✓	✓	✓
Frequency	R/L	A/P	A/P	R/L	A/P
Recommended Hip MRI Protocol at 3.0T (Coil: cardiac, Position : feet first supine)					
	Coronal FMIR Body	Axial FSE Body	Sagittal FSE	Coronal FSE	Oblique axial FSE
TR (msec)	4000–5000	2500	3500–4000	4000	4000
TE (msec)	16	27	26	26	27
TI (msec)	190				
BW (kHz)	62.5	62.5	62.5	62.5	62.5
ETL	12–18	8–12	12	18	12
Flip (deg.)					
NEX	1	2	2	2	2
FOV (cm)	Greater inter-trochanteric distance plus 2cm	Greater inter-trochanteric distance	17–18	17–18	17–18
Matrix	288 × 192	512 × 256–320	512 × 384–416	512 × 384–416	512 × 320–416
Slice/Gap (mm)	5/0	5/0	2–2.5/0	3–3.5/0	3/0
NPW	✓	✓	✓	✓	✓
Frequency	R/L	A/P	A/P	R/L	A/P

FSE = fast spin echo; TR = repetition time; TE = echo time; TI = time to inversion; BW = receiver bandwidth (over entire frequency range); ETL = echo train length; NEX = number of excitations; FOV = field of view; NPW, no phase wrap.

The axial images are similar to computerized tomography, demonstrating the cartilage over the anterior and posterior walls as well as the bare area of the acetabulum. Careful scrutiny of the fat planes of the bare area should be made to discern small loose bodies. The iliopsoas tendon may be seen in cross-section, and the sciatic, femoral, and obturator nerves may also be well visualized.

In addition to high resolution surface coil images, larger field of view body coil images are recommended, including a coronal fast short tau inversion recovery (STIR) and axial fast spin echo techniques. These latter two pulse sequences are helpful to detect the presence of occult sacral or pubic fractures, which may simulate hip pain in an older individual (insufficiency fracture), or additional pelvic soft tissue masses that may refer pain to the groin, including adnexal masses in women and hernias in men. Larger field of view imaging is also recommended to demonstrate any additional foci of marrow infiltration, such as the presence of metastatic disease.

CARTILAGE AND LABRAL EVALUATION

Complete preservation of joint space on standardized radiographs does not preclude the presence of symptomatic full thickness cartilage defects seen on an appropriately performed MRI. Osteoarthritis of the hip commonly presents with actively delaminating cartilage with flap formation. Unstable, delaminating cartilage is manifest as signal hyperintensity in the basilar components, adjacent to the cartilage bone interface, where the water should be restricted and the relaxation time shortest (Fig. 2A,B). Synovitis, when present, should be noted, as this may indicate a patient that will respond favorably to an intracapsular injection of anti-inflammatory agents, including corticosteroids.

Traumatic injury may also result in shearing of cartilage, particularly in the setting of a posterior subluxation event (2). In a posterior subluxation event, there is an initial fracture through the posterior wall or fracture through the interface of the posterior labrum and the wall; subsequent relocation results in chondral shear over the femoral head as well as a split in the anterior labrum (Fig. 3). Careful scrutiny of the images should be performed for the presence or absence of the low signal intensity tidemark/subchondral bone plate will differentiate between an isolated chondral shear versus an osteochondral fracture, respectively. Osteochondral fractures, given the attached bone with its blood supply, are amenable to primary bioabsorbable fixation and restoration of the

Figure 1. Coronal MR image through the mid portion of the right hip demonstrates intermediate signal articular cartilage, contrasted to the low signal intensity labrum (arrowhead). Note the adjacent illiofemoral ligament (black arrow) and gluteus minimus tendon (white arrow), which is minimally frayed.

articular surface of the femoral head (Fig. 4). In severe trauma, MRI may be helpful in assessing the cartilage over Pipkin fractures of the femoral head, and in detecting areas of chondrolysis or subchondral osteonecrosis.

In the setting of developmental dysplasia, there is a characteristically shallow fovea and acetabular dome, leading to compensatory hypertrophy of both the anterior and superior labrum. The degenerative labrum often generates conspicuous ganglion cysts that dissect secondarily into the dome, with a variable amount of cartilage loss (Fig. 5). MRI may be used to distinguish patients who are candidates for periacetabular osteotomy as opposed to arthroplasty. In the presence of severe cartilage loss, the patient is indicated for arthroplasty. In the presence of mild to moderate cartilage loss, as discerned by MRI, the patient may be deemed suitable for periacetabular osteotomy and acetabular reconstruction.

In patients with conditions predisposed to osteoarthritis such as developmental dysplasia of the hip (DDH), more comprehensive assessment of the cartilage may be obtained with the use of quantitative MR techniques. The mechanical properties of cartilage are attributed to the components of the extracellular matrix. Collagen provides the tensile strength of articular cartilage, whereas the hydrophilic proteoglycans provide the compressive strength. Collagen orientation is best assessed using quantitative T2 mapping, which may be applied to the hip joint in patients at risk for developing osteoarthritis (Fig. 6A,B) (3).

Proteoglycan depletion may be assessed using T1 rho or dGEMRIC techniques (4,5). Kim et al studied patients with developmental dysplasia and found that the dGEMRIC index was sensitive to osteoarthritic changes as well as symptoms, as determined by suitable outcome instruments including the WOMAC score (Western Ontario & McMasters University Osteoarthritis Index) (6). In a follow-up study in patients with developmental dysplasia treated with osteotomy, the same investigative group demonstrated that patients who clinically failed osteotomy had more osteoarthritis on radiographs and lower dGEMRIC indices, but the dGEMRIC index was more predictive of clinical failure (7). In an additional study of patients with DDH who had minimal or no osteoarthritis discernible on radiographs, Nishii et al noted that prolongation of T2 was seen in the majority of early OA patients (8).

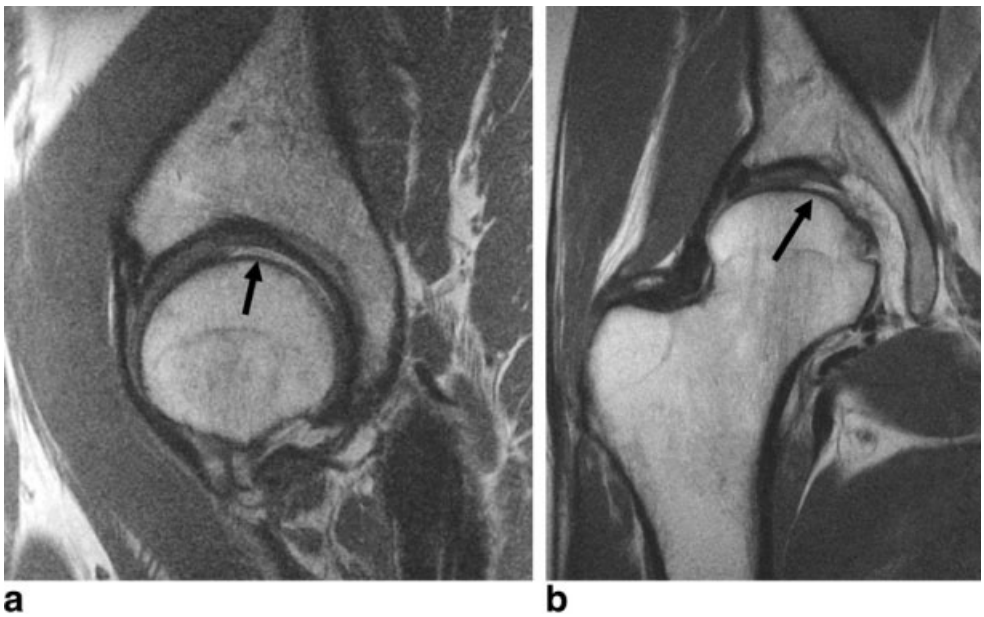

Figure 2. A,B: Sagittal (**A**) and coronal (**B**) MR images of a 53-year-old woman with preserved joint space on radiographs demonstrate active cartilage delamination (arrow on A) with large flap formation over the femoral head and an adjacent defect (arrow on B).

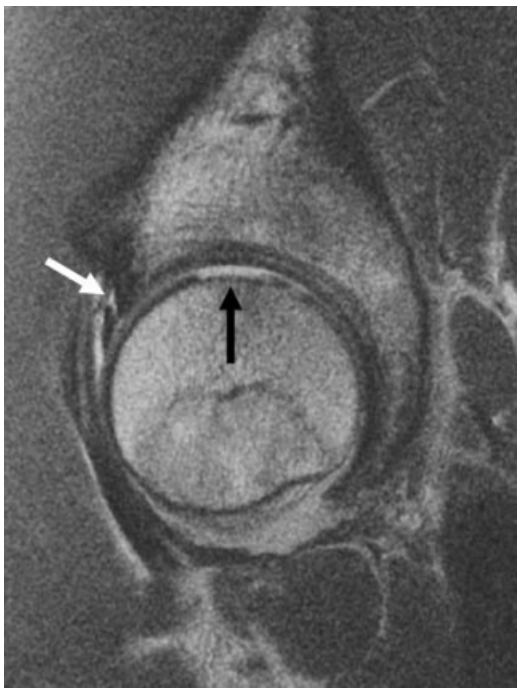

Figure 3. Sagittal MR image of a 19-year-old man 2 days after a posterior subluxation demonstrates a large chondral shear (black arrow) and an adjacent anterior labral tear (white arrow). Note the presence of the low signal tidemark and subchondral plate, indicative of a chondral shear as opposed to an osteochondral fracture.

Figure 4. Coronal MR image of a 17-year-old woman after a transient posterior subluxation demonstrates an osteochondral fracture at the suprafoveal region of the femoral head (arrow). Note the loss of the low signal tidemark, indicative of osteochondral fracture, which was primarily repaired with bioabsorbable pins.

One of the conditions that clearly predisposes patients to hip osteoarthritis at a young age is femoroacetabular impingement syndrome (9). While this condition was initially divided into two types, the cam and the pincer type, most patients present with features of both types. The cam type results from an insufficient offset of the neck–head junction, sometimes implicated by a subclinical subcapital femoral epiphysis. In the cam type, cartilage loss is typically rapid and noted over the anterosuperior margin of the dome. Active delamination may be seen, such that at arthroscopy cartilage is present but unstable, allowing for the arthroscopist to débride fragments of cartilage down to bone. On a preoperative MRI, this is manifest as hyperintensity in the anterior margin of the joint extending down to the tidemark (Fig. 7).

Pincer impingement results from extensive acetabular coverage over the femoral head. The "overcoverage" can be global, as seen in the setting of coxa profunda, or focal at the anterior margin, as is seen in acetabular retroversion. This results in abutment of the femoral neck–head junction against the acetabular rim, impacting the labrum when the hip is placed into flexion. Intralabral ossification is a prominent feature noted at both the lateral margin of the dome and the anterior margin of the hip joint (Fig. 8A,B).

Measurements for insufficient offset at the neck–head junction have been described using MRI, including the alpha angle obtained off of oblique axial MR images, with normal values less than or equal to 55 degrees. Oblique axial MR imaging is recommended, obtained off of a coronal image and parallel to the long axis of the femoral neck, resulting in a long axis view of the neck–head junction, and provides helpful

Figure 5. Coronal MR image of a 27-year-old woman considered for periacetabular osteotomy demonstrates moderately severe acetabular dysplasia, minimal chondral loss, and a chronically torn degenerated labrum yielding a ganglion cyst (arrow).

Figure 6. A,B: Sagittal fast spin echo (**A**) and correlative T2 mapping (**B**) of a 27-year-old man with symptomatic femoroacetabular impingement demonstrate prolonged T2 relaxation in the articular cartilage over the femoral head (B). T2 images are color-coded to capture T2 values from 10 to 90 ms, with green values reflecting longer T2 values. Note the intralabral ossification in the anterior labrum (arrow in A).

information for preoperative planning and subsequent arthroscopic osteochondroplasty (Fig. 9). Using the alpha angle, a line is drawn between the center of the femoral neck at its narrowest point and the center of the femoral head. A second line defining the angle is drawn from the center of the femoral head to the point where the bony "bump" exceeds the radius of the femoral head (10,11). Of note, proliferative bone formation may occur both anteriorly and posteriorly over the femoral neck, and the oblique axial images are very helpful in outlining the extent of bone formation that requires removal at the time of arthroscopic debridement (Fig. 10).

Treatment of femoroacetabular impingement typically includes rim debridement (removal of the ossified labrum), arthroscopic osteochondroplasty, and labral debridement and/or reconstruction and repair. Consequences of a neck debridement in an osteoporotic patient include insufficiency fractures, given that the femoral neck becomes narrower, resulting in a stress riser and risk for the development of fracture (Fig. 11).

As femoral retroversion may be seen in the setting of femoroacetabular impingement, standardized assessment of femoral version may be performed during the MR examination. Standardized axial body coil images are suitable for obtaining the angle between a line connecting the center of the femoral head to the center of the femoral neck and the horizontal of the image. This initial angle must then be corrected for the degree of femoral rotation, which requires an additional low resolution body coil image through the distal femoral condyles. If the patient's distal femur lies in internal rotation, the angle obtained from the posterior margin of the femoral condyles relative to the horizontal must be added to the angle obtained more proximally through the hips. If the patient's femur lies in external rotation, the angle obtained from the posterior margin of the distal femoral condyles relative to the horizontal must be subtracted from the angle obtained more proximally. This gives one a corrected assessment of femoral version (normal 12–15 degrees of anteversion) (Fig. 12A,B). Acetabular retroversion is still best assessed on an anteroposterior radiograph of the pelvis rather than MRI (12).

Some controversy exists regarding the use of intra-articular contrast agent to evaluate the labrum and articular cartilage on MRI. Review of the literature comparing contrast and noncontrast MRI demonstrates a range of accuracy for both labrum and

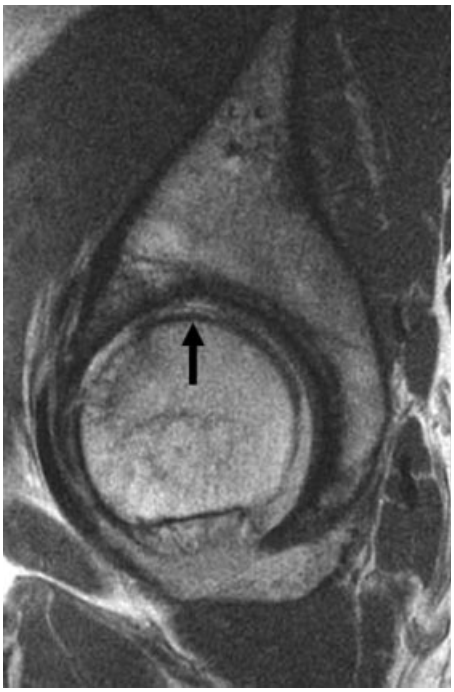

Figure 7. Sagittal MR image of a 45-year-old man with chronic femoroacetabular impingement demonstrates actively delaminating cartilage over the femoral head (arrow) and adjacent subchondral collapse.

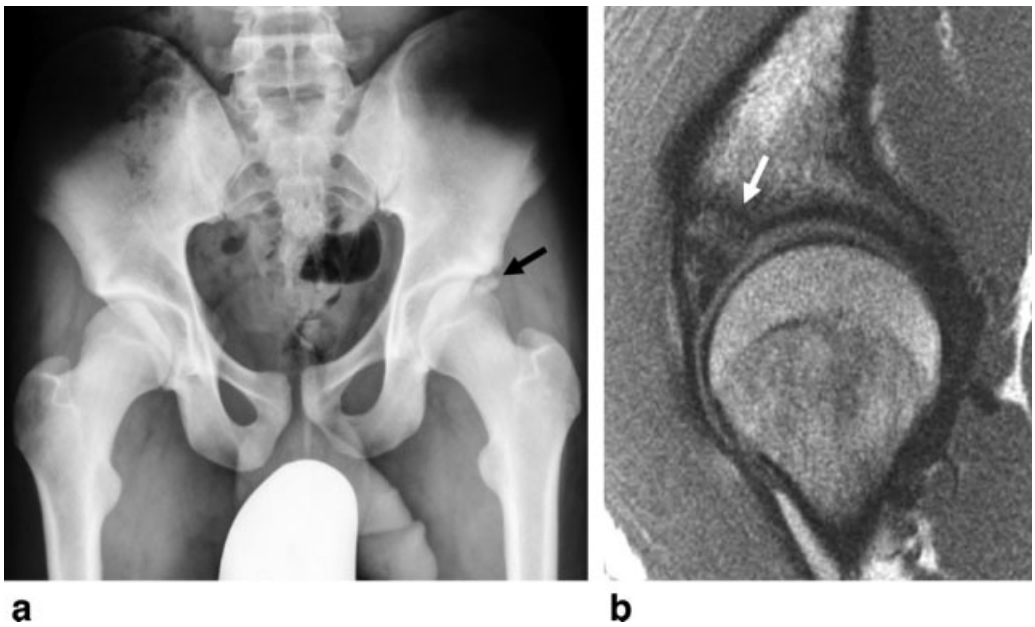

Figure 8. A,B: AP pelvis radiograph (**A**) and sagittal MR image (**B**) of an 18-year-old man with femoroacetabular impingement demonstrate chronic fracture through intralabral ossification (arrows) with adjacent stress reaction in the acetabular dome.

cartilage. With hip arthroscopy as the standard, Keeney et al assessed over 100 consecutive patients with MR arthrography; MR arthrography was noted to have a sensitivity of over 71% and an accuracy of 69% with respective to labral pathology (13). Articular cartilage assessment was less effective, with a sensitivity of 47% and accuracy of 67% (13). Other investigators have demonstrated increased cartilage lesion conspicuity using 3D double echo steady state MR arthrography compared with standardized T1-weighted spin echo MR arthrography; however, similar accuracy was encountered for both sequences using arthroscopy as the standard (14).

One of the advantages of MR arthrography has been the ability to assess the response to intra-articular injection of anesthetic agents, which has been described as having high predictive value for detecting the presence of intra-articular abnormality (15). In this latter study, however, MR arthrography demonstrated a sensitivity of 41% as opposed to 18% for noncontrast MRI (15). In an additional study, Schmid et al evaluated 42 MR arthrograms in 40 patients with a clinical diagnosis of femoroacetabular

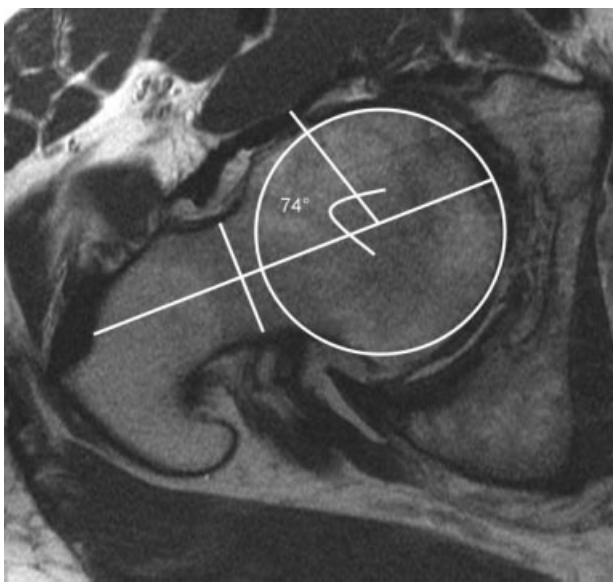

Figure 9. Oblique axial MR image demonstrates an enlarged alpha angle of 74 degrees (Normal alpha angle $\leq 55°$). The alpha angle is defined as the angle between a line intersecting the center of the femoral head and center of the femoral neck at its narrowest point, and a second line drawn from the center of the femoral head to the point where the proliferative bone formation exceeds the radius of the femoral head.

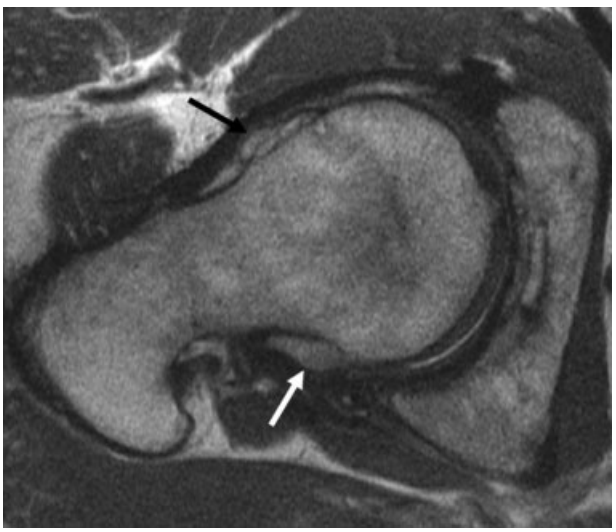

Figure 10. Axial MR image of a man with chronic femoroacetabular impingement demonstrates both anterior (black arrow) and posterior (white arrow) proliferative bone formation.

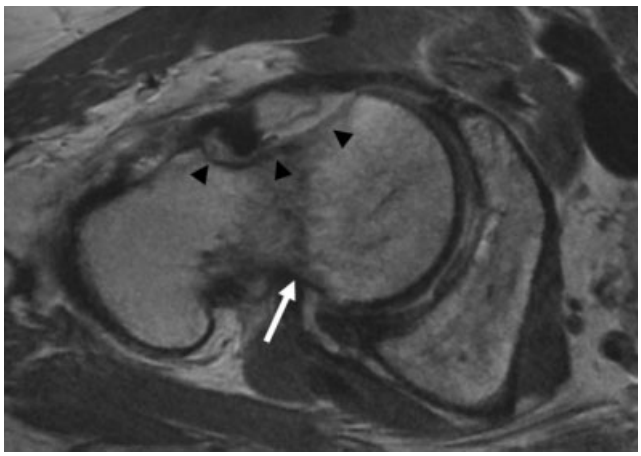

Figure 11. Oblique axial MR image of a 51-year-old woman with femoroacetabular impingement and osteoporosis 1 month after neck debridement (arrowheads) demonstrates a femoral neck fracture (arrow).

impingement and noted that MR arthrography had a sensitivity of 79% with a specificity of 77% (16). In the latter study, interobserver agreement for detection of cartilage in the femoral head was fair with a kappa of 0.31, and relatively poor (less than or equal to 0.2) for evaluation of cartilage in the acetabulum (16).

Of note, diminished spatial resolution in the latter study may be implicated in the inability to achieve acceptable diagnostic performance. More recently, Mintz et al evaluated noncontrast MRI in 92 patients, assessing not only the individual grading of the articular cartilage by a modified Outerbridge scale, but also providing interclass correlation with a weighted kappa score. Using arthroscopy as a standard, 88–92% of cases were noted within one grade of arthroscopy, yielding an accuracy in the cartilage over the femoral head of 87% with a weighted kappa of 0.8 ($P < 0.001$), and an accuracy over the acetabulum of 88% with a weighted kappa of 0.7 ($P < 0.001$) (17).

Labral tears commonly coexist with the presence of cartilage lesions. The hip labrum is composed of fibrocartilage similar to the meniscus of the knee joint, and labral integrity has been implicated in maintaining the normal biomechanics of the hip joint (18). In the knee joint, meniscal repair is favored over resection to maintain the important role of the meniscus in increasing the contact area and thereby decreasing contact stresses on the articular cartilage. This concept has been transported to the hip labrum. Given that meniscal repair is confined to the vascular zone (19), recent investigation has evaluated the vascularity of the hip labrum. Kelly et al evaluated the vascular supply of the hip labrum and noted that the capsule provided the major vascular contribution to the labrum, but that the labrum overall was relatively avascular (20). Labral tears showed a trend of increased vascularity; thus, agents that could potentially augment regional vascularity may prove helpful in subsequent repair of the labrum, rather than labral resection.

After labral resection and arthroscopy, evaluation of the postoperative labrum should be focused not only on the presence of re-tear of the labrum, manifest as fluid imbibition into a repair site or a displaced fragment, but also the presence of cartilage delamination (Fig. 13A,B). In the setting of repair, an intact repair is noted as a somewhat deformed labrum with suture tracks extending through the dome. Careful scrutiny should be made for the presence or absence of fluid imbibition into the site of the tear.

SYNOVIAL PROLIFERATIVE DISEASE

Patients often present with nonspecific hip pain, describing increasing discomfort with flexion and rotation. There are few clinical features that are indicative of a specific diagnosis. Patients with synovitis often present with night pain and the synovitis may be due to the presence of cartilage delamination and osteoarthritis, but may also be due to specific synovial proliferative disorders. In the presence of a joint effusion on large field of view STIR images, careful evaluation of the pattern of synovitis should be made on higher resolution surface coil techniques. The most commonly encountered synovial peripheral diseases

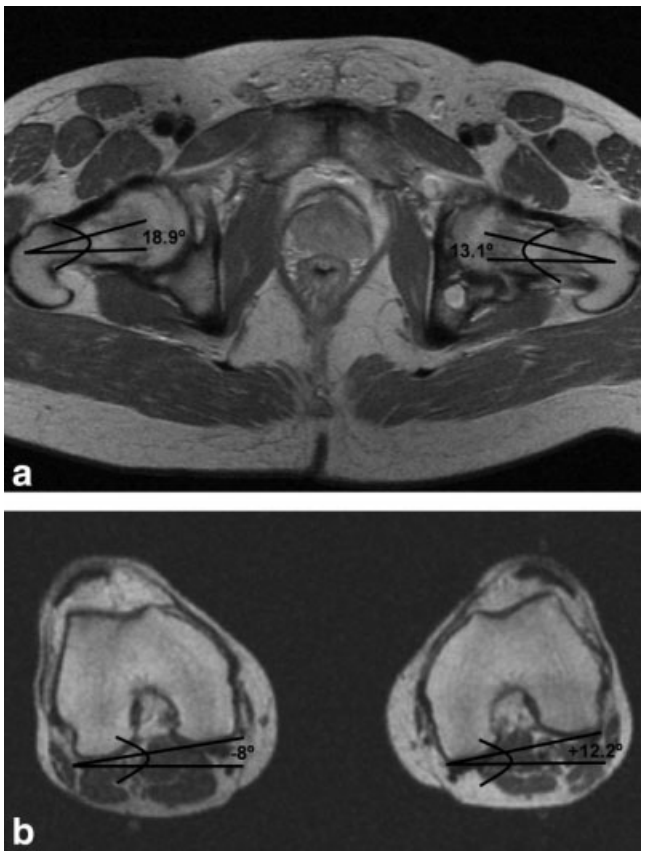

Figure 12. A,B: Axial MR images of the hips (**A**) and knees (**B**) of a 47-year-old man allow for femoral version analysis, corrected for the degree of distal femoral rotation, and demonstrate excessive femoral anteversion on the left measuring 25.3 degrees and 10.9 degrees of right femoral anteversion. Normal femoral anteversion measures 12–15 degrees.

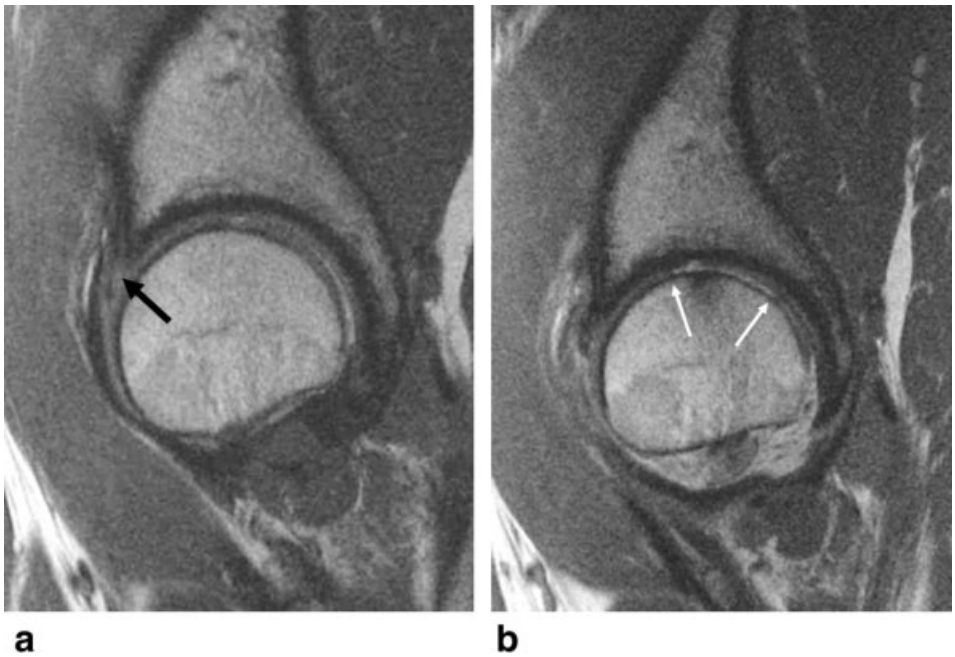

Figure 13. A,B: Preoperative (**A**) and postoperative (**B**) sagittal MR images of ballet dancer with hip pain demonstrate a torn anterior labrum (black arrow), which was resected. The postoperative image obtained less than 2 years later demonstrates markedly progressive cartilage loss from 11:00 to 2:00 (white arrows) with a severe reactive synovitis.

are synovial chondromatosis, in which discrete chondral or osteochondral bodies are identified throughout the capsule, and pigmented villonodular synovitis. In the setting of synovial chondromatosis, the classic MR appearance is that of intermediate signal intensity intracapsular fragments. In the presence of osteochondral bodies, fatty marrow deposits are identified. When the disease becomes confluent, a "cast" of synovium is created, and it may be difficult to discern separate loose bodies. Due to the tight intracapsular pressure of the hip joint, erosions of the femoral neck may be rapid and lead to severe deformity and stress fractures (Fig. 14).

Pigmented villonodular synovitis has two forms: one nodular, appearing as an intracapsular soft tissue mass of intermediate to low signal intensity, and a diffuse form, with diffuse filling of the capsular recesses by intermediate to low signal intensity laden synovium. In the diffuse form, cartilage loss may be rapid. Due to the paramagnetic effect of the hemoglobin degradation products in the synovium, gradient echo techniques may be used to increase diagnostic specificity by improved visualization of the low signal intensity deposits in the synovium (Fig. 15). Preoperative assessment is helpful in discerning the degree of intra- versus extracapsular disease. Extracapsular deposits may decompress outside the joint and compress regional neurovascular structures, simulating spine pathology.

ABDUCTOR TENDINOSIS

Abductor tendinosis has been referred to as "rotator cuff of the hip" (2,1). The integrity of the gluteus medius and minimus tendons should be assessed similar to the rotator cuff tendons in the shoulder, evaluating the signal of the muscle as well as the tendon attachment to the facets of the greater trochanter. Note should be made of the degree of tendon degeneration, partial versus complete tear, as well as the degree of fatty atrophy of the muscle. Disproportionate fatty atrophy due to subselective denervation of the gluteus minimus muscle is not uncommon in the absence of tendon detachment. In addition, when evaluating MR

Figure 14. Coronal MR image of a 46-year-old woman demonstrates profound erosion of the femoral neck due to the presence of synovial chondromatosis (white arrow), creating a chronic stress reaction at the medial margin of the femoral neck (black arrow).

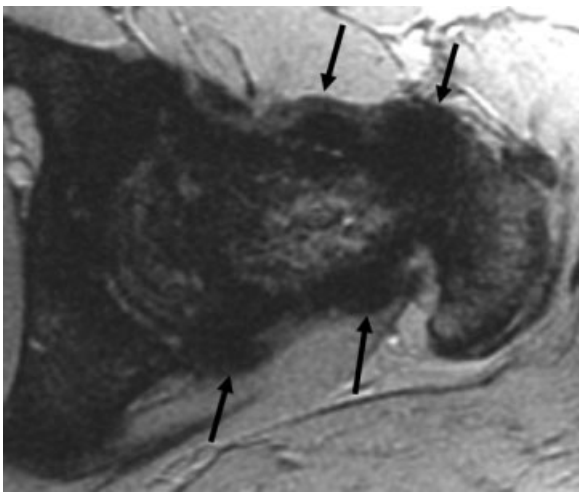

Figure 15. Axial gradient echo MR image in a patient with the diffuse form of pigmented villonodular synovitis (arrows) demonstrates the characteristic low signal intensity synovial deposits due to the paramagnetic effect of hemoglobin degradation products.

images of middle to slightly older aged patients, it is not uncommon to see co-existing anterior labral tears, abductor tendinosis, greater trochanteric bursitis, and some degree of osteoarthritis. In the presence of tendon tears with good muscle quality, primary repairs of the hip abductors may be performed to restore the normal hip mechanics and gait (23).

OSTEONECROSIS

MRI is the most sensitive and specific imaging modality for diagnosing osteonecrosis of the femoral head, with reported sensitivities and specificities as high as 100% (24). The management of osteonecrosis depends on the stage at presentation; thus, early and accurate diagnosis is essential to define appropriate management. The classic appearance of osteonecrosis on MRI is the "double line sign," reflecting the zone of demarcation at the necrotic-viable bone interface, noted as an intermediate to low signal intensity adjacent to an inner band of higher signal intensity (25). Two of the most important variables that affect management include the presence or absence of focal collapse of the femoral head, and the signal characteristics of the subchondral marrow within the necrotic-viable bone interface. The presence of fatty marrow signal within the interface is generally associated with a good prognosis, bone marrow edema pattern presents with a variable diagnosis, and subchondral marrow fibrosis, or low signal intensity on all pulse sequences, is associated with a relatively poor prognosis (25,26). The lack of ability to move water on MRI using appropriate pulse sequences, including fat suppression, indicates completely devitalized marrow that would not be amenable to vascular recruitment surgery such as core decompression or the placement of a vascularized free fibular graft (27) (Fig. 16).

In addition, it is helpful to give an estimate of the degree of involvement of the weight bearing aspect of

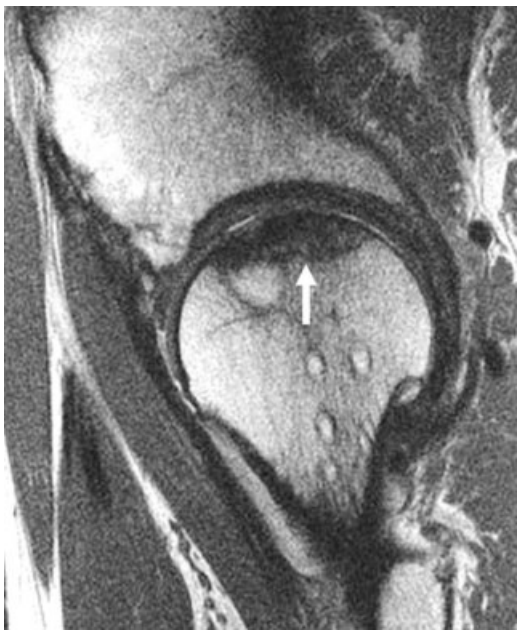

Figure 16. Sagittal proton density MR image of a 52-year-old man with osteonecrosis demonstrates marked low signal intensity marrow (arrow) that remained low signal in STIR images, indicative of devitalized marrow. The patient went on to subsequent collapse and arthroplasty.

the femoral head, as an increased risk of subchondral collapse has been associated with lesions that affect a greater subchondral surface area (27). More sophisticated assessment of the geometry of the femoral head is performed with segmentation algorithms, but these

Figure 17. A,B: Coronal inversion recovery (**A**) and sagittal proton density (**B**) MR images of a 59-year-old man with hip pain demonstrate an intense bone marrow edema pattern due to a subtle subchondral insufficiency fracture (arrows).

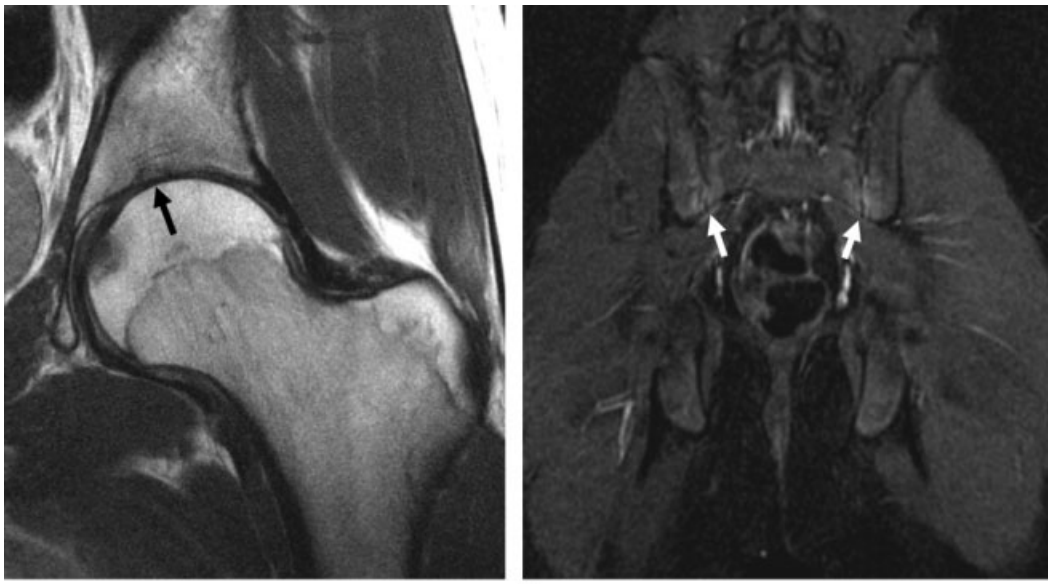

Figure 18. A,B: Coronal proton density (**A**) and STIR (**B**) MR images of a 17-year-old boy, requested to rule out labral tear, demonstrate inflammatory sacroiliitis (white arrows), and diffuse loss of articular cartilage (black arrow), consistent with a spondyloarthropathy. Serologic testing confirmed ankylosing spondylitis.

techniques are usually not necessary for a standardized diagnosis (28).

Distinction between osteonecrosis and subchondral insufficiency fractures is important, as they have a different prognosis. Subchondral fractures often present with a sudden onset of severe pain. The characteristic subchondral fracture is found adjacent and often parallel to the subchondral plate and contour of the femoral head, requiring high resolution techniques (29). One could argue that many of the cases of transient osteoporosis performed on older MR systems with relatively poor spatial and through-plane resolution were subchondral insufficiency fractures, where the fracture line was beyond the resolution of the acquired images (Fig. 17A,B).

CONCLUSIONS

High resolution noncontrast MR imaging may provide reproducible, accurate assessment of cartilage, labrum, and synovium. Strict attention to imaging technique, however, is imperative. Noncontrast techniques allow the advantage of visualizing the native capsule of the hip joint unaltered by intra-articular saline or gadolinium, allowing the imager to scrutinize and distinguish different patterns of synovial proliferation. Noncontrast imaging preserves MRI as a noninvasive diagnostic imaging tool and reduces the cost borne by patients or insurance companies for the use of gadolinium, and also increases patient throughput and unit productivity. The same images are sensitive for cartilage, ligament, tendon, and labral pathology. Finally, hip pain is nonspecific, and despite a clinically directed diagnosis such as "rule out labral tear," the MR radiologist should carefully evaluate the pattern of cartilage loss as well as the structures outside the hip joint to provide an accurate and sometimes clinically unsuspected diagnosis (Fig. 18A,B).

REFERENCES

1. Farjo LA, Glick JM, Sampson TG. Hip arthroscopy for acetabular labral tears. Arthroscopy 1999;15:132–137.
2. Moorman CT III, Warren RF, Hershman EB, et al. Traumatic posterior hip subluxation in American football. J Bone Joint Surg Am 2003;85:1190–1196.
3. Xia Y, Moody JB, Burton-Wurster N, Lust G. Quantitative in situ correlation between microscopic MRI and polarized light microscopy studies of articular cartilage. Osteoarthritis Cartilage 2001; 9:393–406.
4. Bashir A, Gray ML, Boutin RD, Burstein D. Glycosaminoglycan in articular cartilage: in vivo assessment with delayed Gd(DTPA)-2-enhanced MR imaging. Radiology 1997;205:551–558.
5. Reddy R, Insko EK, Noyszewski EA, Dandora R, Kneeland JB, Leigh JS. Sodium MRI of human articular cartilage in vivo. Magn Reson Med 1998;39:697–701.
6. Kim YJ, Jaramillo D, Millis MB, Gray ML, Burstein D. Assessment of early osteoarthritis in hip dysplasia with delayed gadolinium-enhanced magnetic resonance imaging of cartilage. J Bone Joint Surg Am 2003;85:1987–1992.
7. Cunningham T, Jessel R, Zurakowski D, Millis MB, Kim YJ. Delayed gadolinium-enhanced magnetic resonance imaging of cartilage to predict early failure of Bernese periacetabular osteotomy for hip dysplasia. J Bone Joint Surg Am 2006;88: 1540–1548.
8. Nishii T, Tanaka H, Sugano N, Sakai T, Hananouchi T, Yoshikawa H. Evaluation of cartilage matrix disorders by T2 relaxation time in patients with hip dysplasia. Osteoarthritis Cartilage 2008;16:227–233.
9. Ganz R, Parvizi J, Beck M, Leunig M, Nötzli H, Siebenrock KA. Femoroacetabular impingement: a cause for osteoarthritis of the hip. Clin Orthop Relat Res 2003;417:112–120.
10. Notzli HP, Wyss TF, Stoecklin CH, Schmid MR, Treiber K, Hodler J. The contour of the femoral head-neck junction as a predictor for the risk of anterior impingement. J Bone Joint Surg Br 2002; 84:556–560.
11. Pfirrmann CW, Mengiardi B, Dora C, Kalberer F, Zanetti M, Hodler J. Cam and pincer femoral acetabular impingement: characteristic MR arthrographic findings in 50 patients. Radiology 2006;240:778–785.

12. Siebenrock KA, Schoeniger R, Ganz R. Anterior femoro-acetabular impingement due to acetabular retroversion: treatment with periacetabular osteotomy. J Bone Joint Surg Am 2003;85: 278–286.
13. Keeney JA, Peelle MW, Jackson J, Rubin D, Maloney WJ, Clohisy JC. Magnetic resonance arthrography versus arthroscopy in the evaluation of articular hip pathology. Clin Orthop Relat Res 2004;429:163–169.
14. Knuesel PR, Pfirrmann CW, Noetzli HP, et al. MR arthrography of the hip: diagnostic performance of a dedicated water-excitation 3D double echo steady-state sequence to detect cartilage lesions. AJR Am J Roentgenol 2004;183:1729–1735.
15. Byrd JW, Jones KS. Diagnostic accuracy of clinical assessment, magnetic resonance imaging, magnetic resonance arthrography, and intra-articular injection in hip arthroscopy patients. Am J Sports Med 2004;32:1668–1674.
16. Schmid MR, Notzli HP, Zanetti M, Wyss TF, Hodler J. Cartilage lesions in the hip: diagnostic effectiveness of MR arthrography. Radiology 2003;226:382–386.
17. Mintz DN, Hooper T, Connell D, Buly R, Padgett DE, Potter HG. Magnetic resonance imaging of the hip: detection of labral and chondral abnormalities using noncontrast imaging. Arthroscopy 2005;21:385–393.
18. McCarthy JC, Noble PC, Schuck MR, Wright J, Lee J. The watershed labral lesion: its relationship to early arthritis of the hip. J Arthroplasty 2001;16:81–87.
19. Arnoczky SP, Warren RF, Spivak JM. Meniscal repair using an exogenous fibrin clot. J Bone Joint Surg Am 1988;70: 1209–1217.
20. Kelly BL, Shapiro GS, DiGiovanni CW, Buly RL, Potter HG, Hannafin JA. Vascularity of the hip labrum: a cadaveric investigation. Arthroscopy 2005;21:3–11.
21. Bunker TD, Esler CN, Leach WJ. Rotator-cuff tear of the hip. J Bone Joint Surg Br 1997;79:618–620.
22. Kagan A Jr. Rotator cuff tears of the hip. Cin Orthop Relat Res 1999:135–140.
23. Voos JE, Shindle MK, Pruett A, Asnis PD, Kelly BT. Endoscopic repair of gluteus medius tendon tears of the hip. Am J Sports Med 2009;37:743–747.
24. Markisz JA, Knowles RJ, Altchek DW, Schneider R, Whalen JP, Cahill PT. Segmental patterns of avascular necrosis of the femoral heads: early detection with MR imaging. Radiology 1987;162:717–720.
25. Mitchell MD, Kundel HL, Steinberg ME, Kressel HY, Alavi A, Axel L. Avascular necrosis of the hip: comparison of MR, CT and scintigraphy. AJR Am J Roentgenol 1986;146:1215–1218.
26. Sakamoto M, Schimizu K, Iida S, Akita T, Moriya H, Nawata Y. Osteonecrosis of the femoral head: a prospective study with MRI. J Bone Joint Surg Br 1997;79:213–219.
27. Potter HG, Tsou I.The adult hip: magnetic resonance imaging. In: Callaghan JJ, Rosenberg AG, Rubash HE, editors. The adult hip, 2nd edition. Vol. 1. Philadelphia: Lippincott Williams Wilkins; 2007. p 409–422.
28. Hernigou P, Lambotte JC. Volumetric analysis of osteonecrosis of the femur: anatomical correlation using MRI. J Bone Joint Surg Br 2001;83:672–675.
29. Yamamoto T, Kurosaka M, Soejima T, Fujii M. Contrast-enhanced three-dimensional helical CT for soft tissue tumors in the extremities. Skeletal Radiol 2001;30:384–387.